Available online at www.sciencedirect.com
ScienceDirect
Trans. Nonferrous Met. Soc. China 26(2016) 12−18
Transactions of Nonferrous Metals Society of China
www.tnmsc.cn

Microstructure and mechanical properties of cryo-rolled AA6061 Al alloy

Yuan-chun HUANG[1,2,3], Xu-yu YAN[1,4], Tao QIU[3]

1. State Key Laboratory of High Performance Complex Manufacturing, Central South University, Changsha 410083, China;
2. School of Mechanical and Electrical Engineering, Central South University, Changsha 410083, China;
3. Light Alloy Research Institute, Central South University, Changsha 410083, China;
4. School of Materials Science and Engineering, Central South University, Changsha 410083, China

Received 22 February 2015; accepted 24 June 2015

Abstract: The microstructure and mechanical properties of the age hardening AA6061 Al alloy subjected to cryo-rolling (CR) and room temperature rolling (RTR) treatments were investigated. The rolled and aged alloys were analyzed by using DSC, EBSD, TEM, Vickers hardness analysis and tensile test. The results show that the cryo-rolled treatment has an effect on the precipitation sequence of AA6061 Al alloy. The ultrafine grain structures are formed to promote the fine second phase particles to disperse in the aluminum matrix after the peak aging, which is attributed to lots of dislocations tangled in the rolling process. Therefore, the strength and ductility of AA6061 Al alloy are simultaneously modified after the cryo-rolling and aging treatment compared with room temperature rolled one.

Key words: AA6061 Al alloy; cryo-rolling; ultrafine grain structure; disperse distribution; mechanical properties

1 Introduction

Due to the light mass and good mechanical properties [1], aluminum alloys are widely used in vehicle in order to reduce mass and improve fuel economy, especially 6xxx series Al alloy. The mechanical properties of the 6xxx series Al alloy [2,3] could be improved by intermetallic Mg_2Si. But further enhancement of the mechanical properties should be achieved by refining the grain structure to ultrafine grain structure (UGS). The alloys with grain sizes varying from 0.1 to 1 μm [4] have superior mechanical properties compared with the conventional coarse-grained alloys.

In order to obtain ultrafine grain structure, the severe plastic deformation processes [5−9] such as equal channel angular pressing (ECAP), high pressure torsion (HPT) and multiple compression have been extensively researched. But these processes require large amount of plastic and complicated experimental procedures. Cryo-rolling treatment is a new method by deforming at liquid nitrogen temperature (77 K) to produce ultrafine grain structure metals [10−14]. Recent studies [15] have shown that the materials subjected to rolling at liquid nitrogen temperature could suppress dynamic recovery and the density of dislocations would reach a higher steady state level as compared to those rolled at room temperature. As numerous sites for the formation of precipitates, higher densities of dislocations can promote the formation of ultrafine grain structures. Therefore, cryo-rolling treatment greatly improves the mechanical properties of the materials.

However, the application of cryo-rolling treatment to Al alloys has only received limited attention, especially for age hardening Al alloys. So, AA6061 Al alloy subjected to rolling at cryogenic temperature (CR) and room temperature (RTR) was studied in this work. The mechanical properties and microstructure characteristics of the AA6061 Al alloy subjected to cryo-rolling and aging treatments were studied by FE-SEM/EBSD and TEM, respectively.

2 Experimental

The AA6061 Al alloy was procured in the form of

Foundation item: Project (zzyjkt2013-07B) supported by the State Key Laboratory of High Performance Complex Manufacturing, Central South University, China
Corresponding author: Xu-yu YAN; Tel: +86-731-88877315; E-mail: yanxuyu2008@163.com
DOI: 10.1016/S1003-6326(16)64083-9

plates of 10 mm in thickness, with T4 temper state. The chemical composition of the alloy is shown in Table 1. These samples were treated at 520 °C for 1 h and quenched in water and subsequently rolled (at room temperature and liquid nitrogen temperature) from 10 to 1 mm, about 10% reduction per rolling pass. For rolling at liquid nitrogen temperature, the solution-treated plates were dipped in liquid nitrogen for 20 min, and after each pass, the plate was immersed in liquid nitrogen for 5 min before further reduction. Differential scanning calorimetry (DSC) was used to study the precipitates of the AA6061 Al alloy subjected to rolling at different temperatures in order to modify the aging system for AA6061 Al alloy subjected to rolling at different temperatures. To improve the mechanical properties, the cryo-rolled samples were immediately subjected to artificial aging at 100, 130, 150, 180 °C and the room temperature-rolled samples were subjected to artificial aging at 130, 160, 180, 200 and 230 °C with different time (1−24 h), respectively.

Table 1 Chemical composition of AA6061 Al alloy (mass fraction, %)

Si	Fe	Cu	Mn	Mg	Cr	Ti	Al
0.92	0.395	0.263	0.0098	1.01	0.218	0.015	Bal.

Solution treatment was carried out in a box-type furnace, and aging treatment was carried out in a tubular furnace. The strength and ductility of AA6061 Al alloy subjected to different heat treatments were measured by microhardness and tensile tests. Vickers microhardness (HV) was measured by an HV−5 hardness tester on the plane parallel to rolling direction by applying a load of 3 kg for 15 s. The tensile specimens were conducted by using a DDL100 electronic tensile machine operated at a constant displacement speed of 1 mm/min. DSC analysis was carried out in an STA DSC8500 at a heating rate of 10 °C/min from 100 to 320 °C. X-ray diffractometry (XRD) analysis was carried out by a D/MAX2550 diffractometer to identify the precipitates in the AA6061 Al alloy under different processing conditions. X-ray textures were measured on a Bruker D8 Discover texture goniometer. The orientation distribution functions (ODFs) were calculated from incomplete pole figure using the series expansion method with expansion to l_{max}=18 following the formulation of Bunge. Quantitive texture components were calculated by using Texture Calc software. The microstructure features of AA6061 Al alloy with different treatments were analyzed by using a scanning electron microscope (FEI Nova NanoSEM230)/ EBSD analysis and a transmission electron microscope (TEM, JEOL−2100F).

3 Results and discussion

3.1 DSC curves of AA6061 Al alloy

The DSC curves of the AA6061 Al alloy after different treatments are shown in Fig. 1.

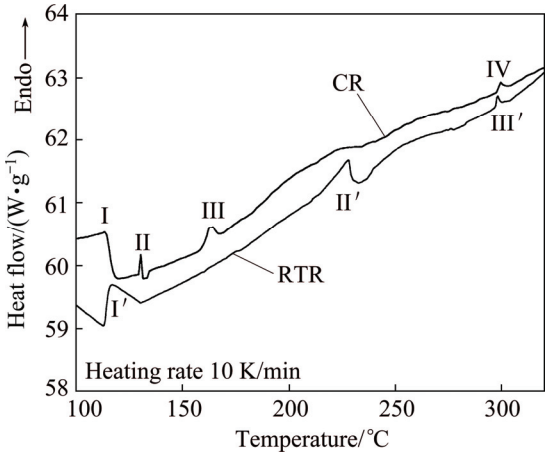

Fig. 1 DSC curves of AA6061 alloy after CR and RTR treatments at different temperatures

It can be seen from Fig. 1 that, for the DSC curve of the CR alloy, there are four exothermic peaks, namely 114 °C (peak I), 130 °C (peak II), 165 °C (peak III) and 300 °C (peak IV). Peak I is related to the formation of GP zones [16]. A large number of dislocations are formed during rolling, which provide stored energy for atomic aggregation. Peak II corresponds to the formation of β'' phase. With increasing temperature, GP zone gradually transforms into β'' phase. With the further increase of temperature, peak III appears and β'' phase gradually transforms into β' phase. Peak IV corresponds to the precipitation of β phase. Therefore, the precipitation sequence of CR AA6061 Al alloy is α (SSS) → GP zones→ β'' phase→ β' phase→ β phase.

The DSC curve of the RTR alloy is different from that of the CR alloy. There are only three exothermic peaks, namely 117 °C (peak I′), 228 °C (peak II′) and 298 °C (peak III′). The reason for the formation of peak I′ is as the same as that of the peak I of CR alloy. Peak II′ is due to the reversion, recrystallization and the formation of β' phase [17]. Peak II′ lags behind peak III, because a large number of dislocations and sub-structures are formed in CR treatment, which accelerate the precipitation of metastable phase (β'' and β' phases). Peak III′ corresponds to the formation of β phase. Therefore, the precipitation sequence of RTR AA6061 Al alloy is α (SSS)→GP zones→ β' phase→ β phase.

3.2 Tensile and hardness properties

In order to obtain the best aging temperature and time for CR alloy and RTR alloy, the CR alloys were

immediately subjected to artificially aging at 100, 130, 150 and 180 °C, and the RTR alloys were subjected to artificial aging at 130, 160, 180, 200 and 230 °C for different time (1−24 h), respectively.

As can be seen from Fig. 2(a), under the condition of aging at low temperature (100 °C), the hardness increases slowly with increasing aging time, but the hardness is smaller than that at other temperatures. For aging at a higher temperature (180 °C), the hardness increases firstly and then substantially decreases with increasing aging time. For aging at the medium temperature (130 and 150 °C), especially at 130 °C, the hardness reaches the maximum and then keeps stable. Combined with the DSC curve of the CR AA6061 Al alloy in Fig. 1, aging at 130 °C corresponds to the formation of β'' phase, aging at 150 °C corresponds to the formation of β' phase. β'' and β' phases can improve the strength of the alloy due to their semi-coherent with aluminum matrix. The hardness of the alloy aged at 150 °C decreases after 20 h, which is attributed to the transformation from β' phase to β phase. The metastable phases of CR alloy at 130 °C are more stable than those in other states. So, the peak aging system for CR alloy is aging at 130 °C for 20 h.

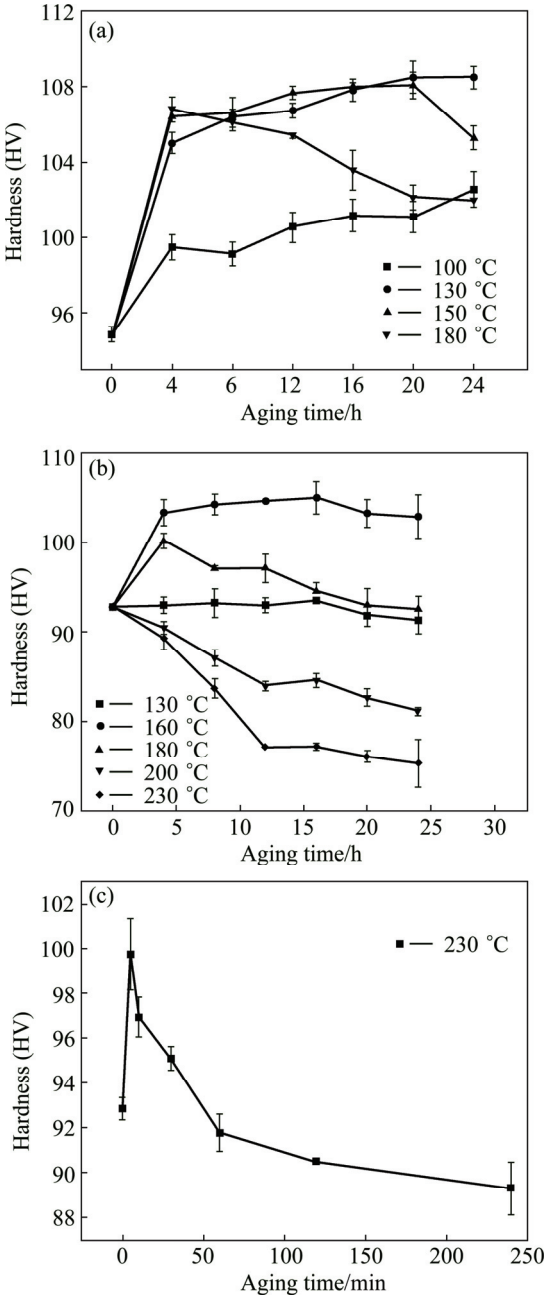

Fig. 2 Vickers hardness vs aging time (0−24 h) at different temperatures for CR AA6061 Al alloy (a) and RTR AA6061 Al alloy (b) and RTR AA6061 Al alloy aged at 230 °C for different time (c)

It can be seen from Fig. 2(b) that the hardness of the RTR alloys presents different changes in comparison with that of the CR ones, especially at high temperatures (200 and 230 °C). The hardness decreases with the processing of aging. In addition, the softening phenomenon becomes more obvious while the temperature gets higher. The hardness changes little under the lower temperature (130 °C); in the meantime, it increases in early 16 h and then substantially declines at a higher temperature of 160 °C. What's more, the hardness of the alloy under 160 °C and 16 h is higher than that in any other state, which is proved to be the peak aging system for RTR alloy. For aging at 180 °C, the hardness appears the same changes as that aged at 160 °C, and the only difference is that the peak value appears at 4 h. The *D*-value of the alloy aged at 160 and 180 °C becomes larger and larger with the extension of aging time. However, the peak aging temperature is not conforming to the DSC curve of the RTR AA6061 Al alloy as shown in Fig. 1, which may be because the higher temperature causes faster phase precipitation [18]. The aging behaviors of the RTR alloy were further studied at 230 °C for 5, 10, 30, 60, 120 and 240 min, respectively, and the results are shown in Fig. 2(c). From Fig. 2(c), the hardness immediately increases at just as long as 5 min, and then drops along with the increase of aging time. At 240 min, the hardness is merely HV 89.29. The RTR alloy can also achieve the peak hardness at 230 °C. But the application to the industrialization is very difficult for short aging time. So, the peak aging system for RTR is aging at 160 °C for 16 h. In contrast, the aging system of the CR alloy is aging at 130 °C for 20 h.

Figure 3 shows the engineering stress−strain curves and tensile properties of AA6061 Al alloy in different states (CR, RTR, CR + aging at 130 °C for 20 h, RTR + aging at 160 °C for 16 h). As can be seen from Fig. 3, mechanical properties of CR alloy in different states are superior to those of RTR alloy. Compared with RTR alloy, the yield strength (YS) of CR alloy increases from 66.40 to 93.61 MPa, and ultimate tensile strength (UTS) increases from 134.7 to 182.07 MPa; while the

elongation (EL) slightly increases by 4.23%. The yield strength and ultimate tensile strength of CR alloy in peak aging condition increase by 52.87% and 32.57%, respectively, compared with RTR+aging at 160 °C for 16 h alloy. In addition, the elongation also increases by 25.94%. Therefore, the mechanical properties of the alloy subjected to cryo-rolling treatment can be significantly enhanced, especially in aging state. KIM et al [19] showed that the AA6061 Al alloy through ECAP and aging treatment only enhanced the strength but not the ductility. Our research shows that CR peak aging significantly improves both the strength and the ductility of AA6061 Al alloy.

3.3 Texture analysis

Figure 4 shows orientation distribution functions (ODF) of the alloys in different states, and Table 2 shows the volume fraction of main texture. It can be seen from Fig. 4 and Table 2 that the S orientation texture has the highest volume fraction in both CR and RTR alloys. The volume fraction of the rolled texture components (Copper, Brass and S) in CR alloy is obviously higher than that of RTR alloy, about 71.95%, while the recrystallization components (Goss, Cube) of RTR alloy is higher than that of CR alloy. Therefore, the cryo-rolling treatment can suppress the recovery and recrystallization during the rolling process.

3.4 Microstructure analysis by EBSD and TEM

EBSD images of grain orientation distribution of alloys subjected to CR and RTR treatments are shown in Fig. 5.

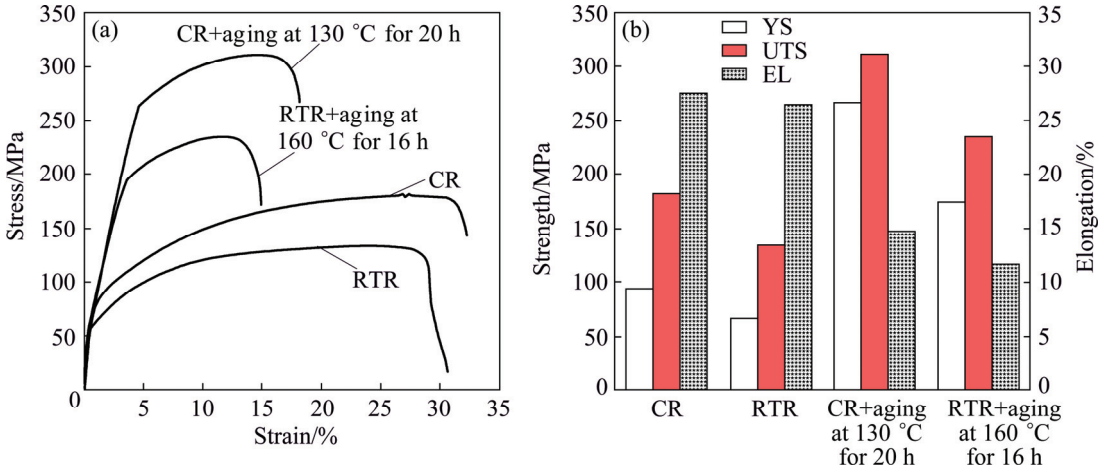

Fig. 3 (a) Engineering stress−strain curves of AA6061 Al alloy in different states (CR, RTR, CR + aging at 130 °C for 20 h, RTR + aging at 160 °C for 16 h); (b) Histogram showing corresponding tensile properties of AA6061 Al alloy in different states

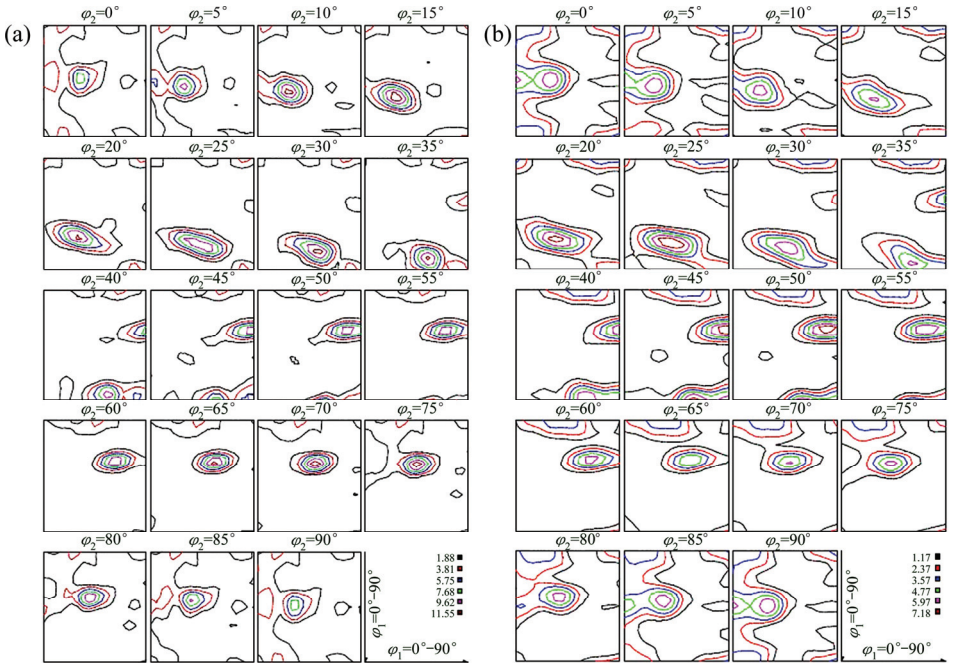

Fig. 4 Orientation distribution functions (ODFs) of AA6061 Al alloys in different states: (a) CR; (b) RTR

Table 2 Volume fractions of main texture components in CR and RTR AA6061 Al alloys (%)

Sample	Rolling texture component			Recrystallization component	
	Copper {112}⟨111⟩	Brass 110}⟨112⟩	S {123}⟨634⟩	Goss {110}⟨001⟩	Cube {001}⟨100⟩
CR	17.13	16.57	38.25	17.65	0.52
RTR	11.79	25.24	26.91	16.06	14.97

It can be seen from Fig. 5(a) that the sub-grains (0.8−0.9 μm) with low angle grain boundary along the rolling direction can be observed in CR alloy. The fragmented and elongated grains are observed along the rolling direction in RTR alloy without sub-grains and the average grains of 5−6 μm are larger than those of CR, as shown in Fig. 5(b).

Figure 6 shows the TEM images in {100} crystal zone axis of the alloy subjected to different treatments. As can be seen from Fig. 6(a), high dislocation densities and dislocation cell structures are observed in CR alloy, which is in a good agreement with the ultrafine grain structures in EBSD images shown in Fig. 5(a). And it can be also seen from Fig. 6(b) that there are lots of dislocations stacking at the grain boundary of RTR alloy. However, dislocations are not formed in the alloys subjected to aging at 130 °C for 20 h and at 160 °C for 16 h. In CR alloy after peak aging at 130 °C for 20 h, fine second phase particles are diffusely distributed in the aluminum matrix (Fig. 6(c)). The grain size of the second

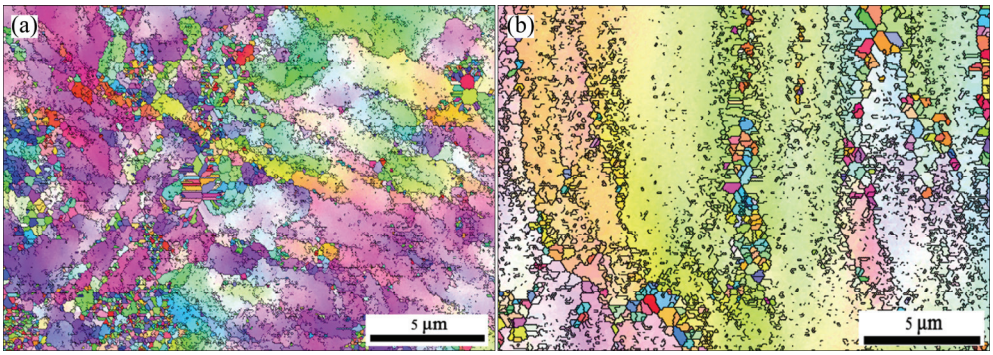

Fig. 5 EBSD images showing grain orientation distribution of AA6061Al alloys after different treatments: (a) CR; (b) RTR

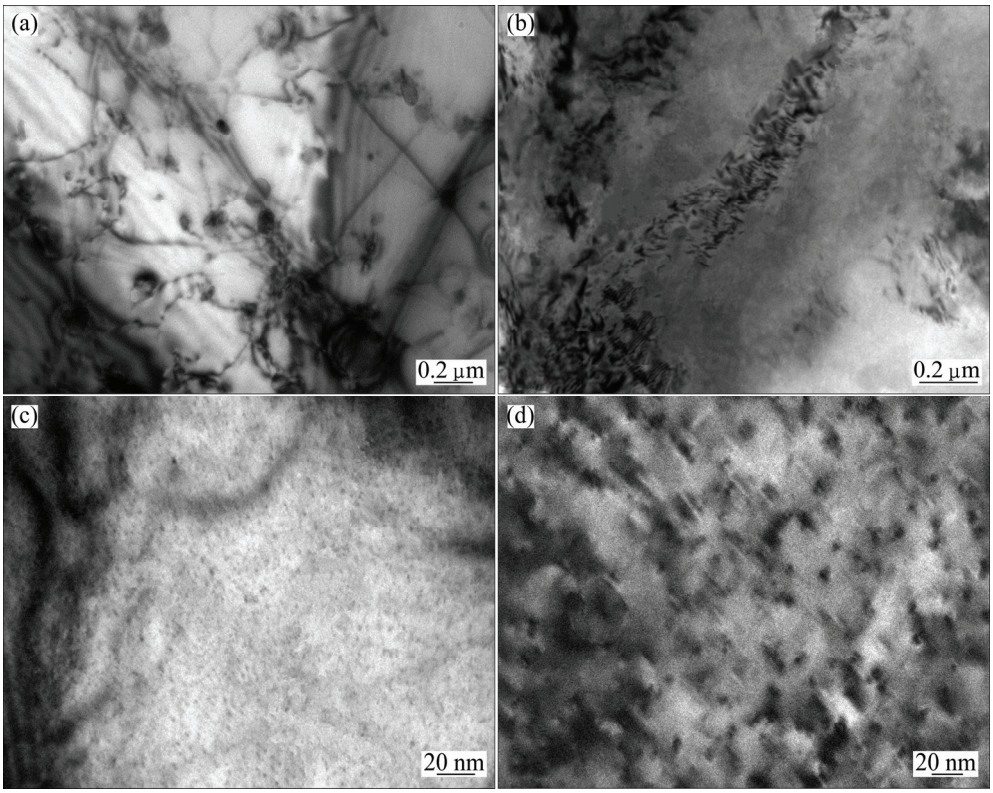

Fig. 6 TEM images in {100} crystal zone axis of AA6061 Al alloy subjected to different treatments: (a) CR; (b) RTR; (c) CR + aging at 130 °C for 20 h; (d) RTR + aging at 160 °C for 16 h

phase particles, Mg_2Si, from XRD data (Fig. 7), in the RTR + aging at 160 °C for 16 h alloy, is larger than that of the CR + aging at 130 °C for 20 h alloy (Fig. 6(d)).

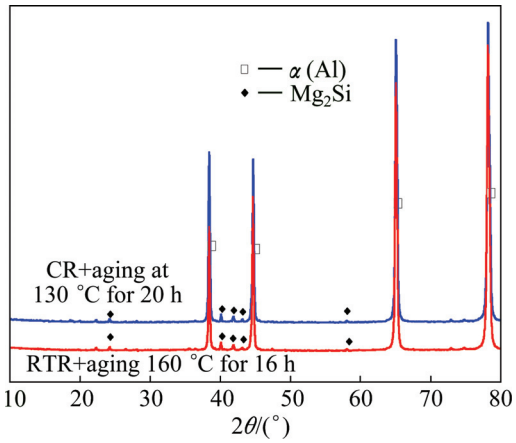

Fig. 7 XRD patterns of AA6061 Al alloy subjected to different treatments

The grain size has a significant influence on the mechanical properties of alloys, which can be explained through Hall–Petch equation [20]:

$$\sigma_y=\sigma_i+k_y d^{-1/2} \quad (1)$$

where σ_i and k_y are constants of alloys, d is the average grain size.

The strength has a functional relation with the grain size. During the rolling process, the CR alloy forms large numbers of the dislocations which tangle to ultrafine grain structure. The dislocations with diffusive distribution in CR alloy provide numerous nucleation sites for the second phase particles, Mg_2Si. Mg_2Si particle is the main strengthening phase [21] in AA6061 Al alloy, which forms in peak aging and is diffusely distributed in the matrix, as shown in the TEM images. High strength of CR + aging at 130 °C for 20 h alloy is due to the fine second phase from the Orowan mechanism [22]. The Orowan mechanism can explain that the fine size of precipitate has the inverse proportion relationship with the critical shear stress. So, the CR alloy after the peak aging possesses higher strength.

Diffuse distribution of precipitates after the peak aging has no significant changes in grain structure, while the ductility is decreased. But with the diffuse distribution and finer second phase particles, the decrease will be small. Compared with RTR + aging at 160 °C for 16 h alloy, CR alloy after peak aging treatment significantly improves the material ductility due to the role of the ultrafine grain structure and second phase particles.

Therefore, the mechanical properties of CR alloy, both in rolling and aging states are superior to those of RTR alloy.

4 Conclusions

1) The cryo-rolling treatment changes the precipitation sequence of AA6061 Al alloy, which accelerates precipitation of metastable phase (β'' phase and β' phase). There is no β'' phase appearing in RTR alloy. The precipitation sequence of CR AA6061 Al alloy is α (SSS) → GP zones→ β'' phase→ β' phase→ β phase; the precipitation sequence of RTR AA6061 Al alloy is α (SSS) → GP zones→ β' phase→ β phase.

2) Cryo-rolling of AA6061 Al alloy with thickness reduction of 90% can improve the mechanical properties (YS of 93.61 MPa, UTS of 182.07 MPa and elongation of 27.56%); cryo-rolled material after peak aging at 130 °C for 20 h shows a significant increase in mechanical properties: YS increase by 52.87%, UTS increase by 32.57% and elongation increase by 25.94%.

3) The volume fraction of rolling texture components (Copper, Brass and S) is 71.95%, which is higher in CR alloy than that of RTR alloy, indicating that cryo-rolling procedure can suppress the recovery and recrystallization in the rolling process.

4) The ultrafine grain structures are formed in AA6061 Al alloy after cryo-rolling treatment, which is attributed to lots of dislocations tangled in the rolling process. The dislocations and ultrafine grain structures with high stored energy promote fine second phase particles to disperse in the aluminum matrix after the peak aging.

References

[1] BURGER G, GUPTA A, JEFFREY P, LLOYD D. Microstructural control of aluminum sheet used in automotive applications [J]. Materials Characterization, 1995, 35(1): 23−39.

[2] SHEN Chen-hui. Pre-treatment to improve the bake-hardening response in the naturally aged Al−Mg−Si alloy [J]. Journal of Materials Science and Technology, 2011, 27(3): 205−212.

[3] PANIGRAHI, SUSHANTA K, JAYAGANTHAN R. A study on the mechanical properties of cryorolled Al−Mg−Si alloy [J]. Materials Science and Engineering A, 2008, 480(1): 299−305.

[4] VALIEV R Z, ISLAMGLIEV R K, ALEXANDROV I V. Bulk nanostructured materials from severe plastic deformation[J]. Progress in Materials Science, 2000, 45(2): 103−189.

[5] SAITO Y, UTSUNOMIYA H, TSUJI N, SAKAI T. Novel ultra-high straining process for bulk materials—Development of the accumulative roll-bonding (ARB) process [J]. Acta Materialia, 1999, 47(2): 579−583.

[6] ZHENG L J, LI H X, HASHMI M F, CHEN C Q, ZHANG Y, ZENG M G. Evolution of microstructure and strengthening of 7050 Al alloy by ECAP combined with heat-treatment [J]. Journal of Materials Processing Technology, 2006, 171(1): 100−107.

[7] HUANG Y, PRANGNELL P B. Continuous frictional angular extrusion and its application in the production of ultrafine-grained sheet metals [J]. Scripta Materialia, 2007, 56(5): 333−336.

[8] RICHERT M, LIU Q, HANSEN N. Microstructural evolution over a large strain range in aluminium deformed by cyclic-extrusion–

compression [J]. Materials Science and Engineering A, 1999, 260(1): 275−283.
[9] ZHILYAEV A P, NURISLAMOVE G V, KIM B K, BARO M D, SZPUNAR J A, LANGDON T G. Experimental parameters influencing grain refinement and microstructural evolution during high-pressure torsion [J]. Acta Materialia, 2003, 51(3): 753−765.
[10] WANG Yin-min, CHEN Ming-wei, ZHOU Feng-hua, MA En. High tensile ductility in a nanostructured metal [J]. Nature, 2002, 419(6910): 912−915.
[11] RANGARAJU N, RAGHURAM T, KRISHNA B V, RAO K P, VENUGOPAL P. Effect of cryo-rolling and annealing on microstructure and properties of commercially pure aluminium [J]. Materials Science and Engineering A, 2005, 398(1): 246−251.
[12] LEE T R, CHANG C P, KAO P W. The tensile behavior and deformation microstructure of cryo-rolled and annealed pure nickel [J]. Materials Science and Engineering A, 2005, 408(1): 131−135.
[13] SHANMUGASUNDRAM T, MURTY B S, SUBRAMANYA S V. Development of ultrafine grained high strength Al−Cu alloy by cryorolling [J]. Scripta Materialia, 2006, 54(12): 2013−2017.
[14] PANIGRAHI S K, JAYAGANTHAN R, PANCHOLI V. Effect of plastic deformation conditions on microstructural characteristics and mechanical properties of Al 6063 alloy [J]. Materials and Design, 2009, 30(6): 1894−1901.
[15] LEE Y B, SHIN D H, PARK K T, NAM W J. Effect of annealing temperature on microstructures and mechanical properties of a 5083 Al alloy deformed at cryogenic temperature [J]. Scripta Materialia, 2004, 51(4): 355−359.
[16] LIU Hong. Development of a novel Al−Mg−Si−Cu−Mn alloy automotive body sheet material [D]. Shenyang: Northeastern University, 2005: 100−111. (in Chinese)
[17] NIRANJANI L, HARI K C, SUBRAMANYA V S. Development of high strength Al−Mg−Si AA6061 alloy through cold rolling and ageing [J]. Materials Science and Engineering A, 2009, 515(1): 169−174.
[18] ALI A M, GABER A F, MATSUDA K, IKENO S. Investigation and characterization of the nanoscale precipitation sequence and their kinetics in Al−1.0%Mg_2Si−0.4%Si−0.5%Cu (wt) alloy [J]. Materials Chemistry and Physics, 2014, 147(3): 461−468.
[19] KIM J K, JENOG H G, HONG S I, KIM Y S, KIM W J. Effect of aging treatment on heavily deformed microstructure of a 6061 aluminum alloy after equal channel angular pressing [J]. Scripta Materialia, 2001, 45(8): 901−907.
[20] WILLIAM D C, DAVID G R. Materials science and engineering: An introduction [M]. 8th ed. Versailles: Aptara, Inc, 2009.
[21] WANG S, MATSUDA K, KAWABATA T, YAMAZAKI T, IKENO S. Variation of age-hardening behavior of TM-addition Al−Mg−Si alloys [J]. Journal of Alloys and Compounds, 2011, 509(41): 9876−9883.
[22] HOU Yan-hui, GU Yan-xia, LIU Zhi-yi, LI Yun-tao. Modeling of whole process of ageing precipitation and strengthening in Al−Cu−Mg−Ag alloys with high Cu-to-Mg mass ratio [J]. Transactions of Nonferrous Metals Society of China, 2010, 20(5): 863−869.

过冷轧制 AA6061 铝合金的显微组织与力学性能

黄元春[1,2,3]，颜徐宇[1,4]，邱 涛[3]

1. 中南大学 高性能复杂制造国家重点实验室，长沙 410083；
2. 中南大学 机电工程学院，长沙 410083；
3. 中南大学 轻合金研究院，长沙 410083；
4. 中南大学 材料科学与工程学院，长沙 410083

摘 要：对时效硬化 AA6061 铝合金分别进行过冷轧制(CR)、室温轧制(RTR)后的显微组织与力学性能进行研究。通过差热分析(DSC)、电子背散射衍射技术(EBSD)、透射电镜(TEM)、维氏硬度测试、拉伸测试等分析手段对轧制态和时效态的合金进行分析。结果表明：AA6061 铝合金经 CR 处理后，第二相析出序列发生改变。合金在过冷轧制中形成大量位错，并发生缠结形成超细晶粒结构，使得峰值时效下第二相粒子在铝基体中更加细小弥散分布。经过冷轧制后轧制态和峰值时效态下的 AA6061 铝合金强度和塑性较室温轧制态合金的都有很大提高。

关键词：AA6061 铝合金；过冷轧制；超细晶粒结构；弥散分布；力学性能

(Edited by Wei-ping CHEN)